

European Geosciences Union General Assembly 2013, EGU

Division Energy, Resources & the Environment, ERE

Upscaled modeling of CO₂ injection and migration with coupled thermal processes

S. E. Gasda^{a*}, A. F. Stephansen^a, I. Aavatsmark^a, H. K. Dahle^b

^aCenter for Integrated Petroleum Research, Uni Research, Allégaten 41, N-5020 Bergen, Norway

^bDepartment of Mathematics, University of Bergen, Allégaten 41, N-5020 Bergen, Norway

Abstract

A practical modeling approach for CO₂ storage over relatively large length and time scales is the vertical-equilibrium model, which solves partially integrated conservation equations for flow in two lateral dimensions. We couple heat transfer within the vertical equilibrium framework for fluid flow, focusing on thermal processes that most impact the CO₂ plume. We investigate a simplified representation of heat exchange that also includes transport of heat within the plume. In addition, we explore available CO₂ thermodynamic models for reliable prediction of density under different injection pressures and temperatures. The model concept is demonstrated on simplified systems.

© 2013 The Authors. Published by Elsevier Ltd. Open access under [CC BY-NC-ND license](https://creativecommons.org/licenses/by-nc-nd/4.0/).
Selection and peer-review under responsibility of the GFZ German Research Centre for Geosciences

Keywords: geologic CO₂ sequestration; numerical modeling; CO₂ density; PVT formulations; cubic equations-of-state; non-isothermal fluid flow; vertical equilibrium model; sharp-interface; upscaling

1. Introduction

CO₂ migration in the deep subsurface involves physical and thermal processes that occur at multiple spatial and temporal scales. These mechanisms can play an important role in the security of underground CO₂ storage, in particular, the coupling between thermal and geomechanical processes that can lead to fracturing and loss of caprock integrity [1]. Additionally, a better understanding of thermal impact on CO₂ properties is essential for reliable simulation of temperature-related plume dynamics at the field scale

* Corresponding author. Tel.: +47-555-83394; fax: +47-555-88265.
E-mail address: sarah.gasda@uni.no.

[2]. Mathematical models and subsequent simulation must capture the relevant processes at length and time scales appropriate for CO₂ storage, however, the handling of multiple physics over several disparate scales in an efficient manner remains a computational challenge [3].

In this paper, we present the vertical equilibrium (VE) model for coupled thermal processes. The VE model allows for partial integration of the three-dimensional equations, thus greatly reducing the computational effort involved. The two-dimensional horizontal flow equations can be then solved analytically, semi-analytically and numerically [3]. The latter allows for the greatest flexibility regarding horizontal heterogeneity in the geological and fluid properties. The integrated model has been developed recently to include a capillary fringe [4] and subscale structural [5] and solubility trapping [6]. In this work, we extend the VE model for non-isothermal systems by coupling the horizontal flow with energy transport.

Nomenclature

C_{Σ}	total compressibility [1/Pa]
$C_{\Sigma,\theta}$	total heat expansion coefficient [1/K]
C_{th}	total specific heat capacity [J/kg/K]
H	thickness of storage aquifer [m]
P	coarse-scale pressure located at a reference datum [Pa]
P_c	coarse-scale capillary pressure [Pa]
R	specific gas constant [J/kg/K]
Q	mass rate source/sink [kg/s]
S	depth-integrated saturation [-]
$U_{ }$	depth-integrated volumetric phase flux in lateral direction [m ² /s]
a	coefficient in general cubic equation of state
b	coefficient in general cubic equation of state
h	specific phase enthalpy [J/kg]
v	specific volume [m ³ /kg]
Θ	temperature [K]
Ψ	energy source/sink [J/kg/s]
α	subscript to indicate phase; $\alpha = c$ (CO ₂), b (brine), or s (solid)
α_B	bulk compressibility of medium [1/Pa]
β	phase compressibility [1/Pa]
δ_1	parameter in general cubic equation of state
δ_2	parameter in general cubic equation of state
η_c	thickness of CO ₂ plume [m]

θ	dipping angle of aquifer [°]
ρ	phase density [kg/m ³]
ϕ	porosity [-]

2. Vertical equilibrium model

We consider non-isothermal flow of two fluid phases in a porous medium. The fluids consist of a lighter CO₂ phase and denser brine phase. The fluids and rock matrix are compressible. Mineral reactions and mutual solubility are ignored. The VE sharp-interface model is applied to this system, which is based on the following assumptions:

- aspect ratio of the domain is large;
- fluids are segregated due to gravity;
- capillary fringe characteristic length compared with aquifer height is negligible;

The above list implies that vertical flow can be neglected, and therefore pressure is in equilibrium vertically and the vertical saturation profile is well defined. This greatly simplifies the resulting integrated flow and heat transport equations. The VE model presented here consists of a horizontal compressible flow equation that is coupled with a vertically integrated energy flow equation.

2.1. Compressible fluid flow

Applying the VE assumptions, subsequent integration of the fine-scale 3D mass conservation equations results in the following mass conservation equation for each fluid phase,

$$H \frac{\partial (\phi \rho_\alpha S_\alpha)}{\partial t} + \nabla_{\parallel} \cdot (\rho_\alpha \mathbf{U}_{\parallel\alpha}) = Q_\alpha, \quad \alpha = c, b. \quad (1)$$

Let the total compressibility be defined as,

$$C_{\Sigma\alpha} = \frac{\phi}{\rho_\alpha} \frac{\partial \rho_\alpha}{\partial p} + \frac{\partial \phi}{\partial p} = \phi \beta_\alpha + (1 - \phi) \beta_s + \alpha_B. \quad (2)$$

The mass conservation equations can then be combined to obtain a pressure equation that solves for coarse-scale pressure P at the bottom of the reservoir,

$$H [S_c C_{\Sigma c} + (1 - S_c) C_{\Sigma b}] \frac{\partial P}{\partial t} + H S_c C_{\Sigma c} \frac{\partial P_c}{\partial t} + H S_c C_{\Sigma \Theta} \frac{\partial \Theta}{\partial t} + \nabla_{\parallel} \cdot (\mathbf{U}_{\parallel c} + \mathbf{U}_{\parallel b}) = Q_\Sigma, \quad (3)$$

where the source term is the sum over both fluid phases. Here, we have used the VE assumption so that $p_a(z) = P_a - \rho_a g \cos \theta z$. Then, P_c becomes the coarse-scale capillary pressure, defined as $P_c = -\Delta\rho(1-\eta_c)Hg\cos\theta$. The multiphase extension Darcy's law is used for volumetric phase fluxes.

In the development of the pressure equation, further simplifications have been made regarding fluid and matrix properties:

- Rock permeability, porosity and relative permeability are vertically homogeneous;
- Brine phase is slightly compressible due to pressure;
- Velocity of solid surface is slow compared to fluid flow;
- Vertical CO₂ density changes within the plume are neglected;

These assumptions may be relaxed if necessary.

2.2. Energy transport

The integrated energy conservation is written in terms of temperature, which is appropriate if changes in enthalpy and temperature are relatively small [3]. The following assumptions are made:

- no fluid phase changes;
- temperature of solid and fluid phases is in equilibrium locally;
- thermal conductivity can be neglected;
- brine temperature is constant;
- vertical temperature changes within CO₂ plume are negligible, i.e. $\Theta(x,y,z,t)=\Theta(x,y,t)$;
- negligible impact of pressure on energy transport;

The resulting energy balance equation becomes,

$$HC_{th} \frac{\partial \Theta}{\partial t} + \nabla_{\parallel} \cdot (h_c \rho_c \mathbf{U}_{\parallel c}) = \Psi_c, \quad (4)$$

where the total specific heat capacity is defined as,

$$C_{th} = \frac{\partial}{\partial \Theta} (h_c \phi \rho_c - h_s (1 - \phi) \rho_s). \quad (5)$$

2.3. Numerical solution

The coupled system of equations (1), (3), and (4) is solved using an IMPES (Implicit Pressure Explicit Saturation) type solution strategy. The pressure equation (3) is solved implicitly using finite-difference spatial discretization. Then, the temperature (4) and CO₂ saturation (1) are solved explicitly in a sequential manner. A volume correction is used in the pressure equation to account for small volume balance errors that occur when conserving mass in the compressible case.

3. Improved cubic equation of state for CO₂

Cubic equations of state may be written in the form [7],

$$P = \frac{R\Theta}{v-b} - \frac{a(\Theta)}{(v-\delta_1 b)(v-\delta_2 b)}, \quad (6)$$

where $\delta_1 < \delta_2$. Special cases of this cubic equation of state are the Peng-Robinson equation with parameters $\delta_1 = -(\sqrt{2}+1)$ and $\delta_2 = (\sqrt{2} - 1)$ and the Soave-Redlich-Kwong equation with $\delta_1 = -1$ and $\delta_2 = 0$. Also the van der Waals equation is a special case of this form with $\delta_1 = \delta_2 = 0$ and $a(\theta)$ independent of θ , although it does not satisfy the required inequality for δ_1 and δ_2 .

The parameters δ_1 and δ_2 may be chosen to give an equation of state with an improved accuracy for a given substance in a given region of temperature and pressure. As an example is shown the case with $\delta_1 = -3.8$ and $\delta_2 = 0.9$. This case of the cubic equation of state is compared with the Span-Wagner equation [8] for CO₂ for temperatures in the interval 300–310 K and pressures in the interval 7–8 MPa. Curves of equal density are shown in Figure 1 for the values 250, 300, 350, 400, 450, 500, 550, 600, 650 and 700 kg/m³, with the 250 curve at the right-bottom and the 700 curve at the left-top. The density curves are fairly good for the liquid and supercritical domains, but there are larger deviations in the vapor domain. Also, the saturation curve shows a deviation in the lower part.

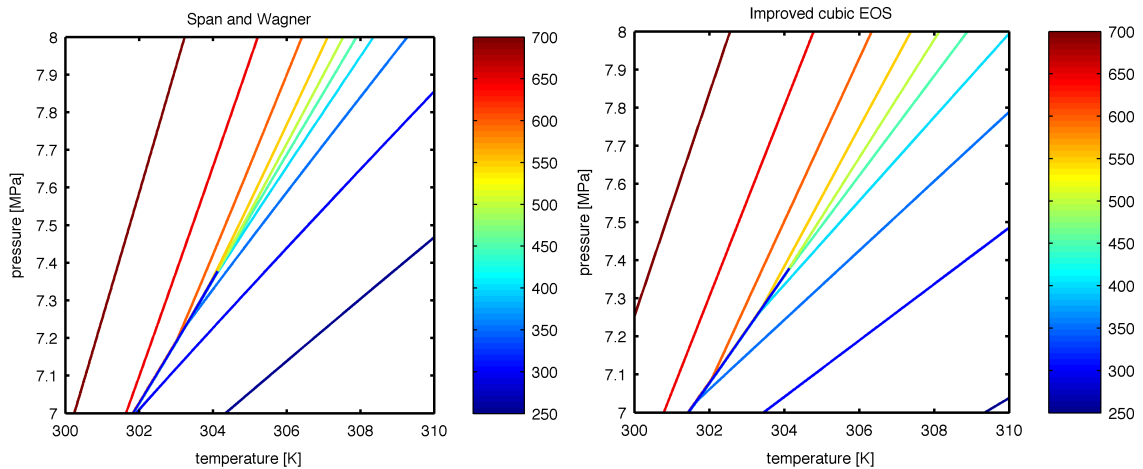


Fig. 1. CO₂ density contours computed near the critical point for two equations of state: (a) Span and Wagner; (b) cubic equation of state with improved coefficients.

4. Application

The non-isothermal VE model presented in Section 3 was applied to two CO₂ injection and migration scenarios. The first represents CO₂ migration in a sloping aquifer due to buoyancy and subject to a geothermal gradient. The temperature conditions are typical of North Sea aquifers, which could bring CO₂ close to the critical point where density is most sensitive to small changes in temperature. The second test case represents injection of CO₂ at a colder temperature than reservoir conditions. This case is also representative of injection of CO₂ that has been transported a long distance along the sea floor before being pumped into the aquifer. These cases demonstrate the impact of CO₂ density on plume evolution over relatively short and long temporal and spatial scales.

4.1. Sloping aquifer

CO₂ migrates in a saline aquifer in a postinjection situation. The saline aquifer is bounded top and bottom by impermeable boundaries. The aquifer is modeled as a 10-m wide cross-section with fixed θ

and P conditions at the upslope boundary. All rock and fluid properties are given in Table 1. CO₂ properties are calculated according to Span and Wagner [8]. CO₂ is emplaced as a fully saturated square initial condition 2.5 km in width and centered at $x = 6.25$ km. The simulation time is 5000 yrs.

Table 1. Aquifer geometry, rock and fluid properties for sloping aquifer simulation case.

Parameter	Value	Units
Aquifer extent	100	m
Aquifer thickness	50	m
Dip angle	1	°
Top surface depth	1800-800	m
Permeability	130	mDarcy
Porosity	15	%
Geothermal gradient	35.6	C/km
Surface temperature	7	C
Brine density	1010.6	kg/m ³
Brine viscosity	0.6	cP
Brine compressibility	0.46	GPa ⁻¹
Rock specific heat capacity	920	J/kg/K
Rock density	2650	kg/m ³
Rock bulk compressibility	0.3	GPa ⁻¹

Two cases of CO₂ density variation are simulated: 1) variable density according to P and Θ , and initial Θ equal to reservoir temperature; and 2) constant density of 570 kg/m³. The initial density and temperature profiles are given in Figure 2a.

After 5000 years (Figure 2b), the two cases show that there is only a slight overestimation of plume speed when assuming a constant density (case 2) compared with density variation in equilibrium with aquifer conditions (case 1). A larger domain extending further upslope would lead to larger discrepancy between the results because the density begins to change rapidly once the plume passes 80 km, which corresponds to 1000-m depth.

4.2. Injection of cold CO₂

The saline aquifer is horizontal and extends 20 km in lateral extent. The top surface lies uniformly at a depth of 1800 m, while the initial temperature is uniform at 70 C. The system is modelled as radially symmetric with fixed Θ and P boundary conditions. The aquifer and fluid properties are the same as given in Section 4.1. CO₂ is injected at a rate of 1 Mtons/yr with a temperature of 20 C into the center of the domain for 5 years. A comparison with CO₂ injected at reservoir temperature is performed.

The results (Figure 3) show a large difference in plume shape in the first 250 km away from the injection well. The cold CO₂ injection leads to a compact plume near the well that expands as temperature increase away from the well. The reservoir temperature case has a more classical conical shape to the plume. The density variation is greatest for the cold CO₂ case, varying from over 900 kg/m³ to nearly 600 kg/m³, which is mostly due to temperature variation. It is interesting to note the increase in temperature near the well for the CO₂ injection at reservoir conditions, which could be due to a pressure increase of 25

bar that causes an energy increases as the CO₂ compresses. However, the increased energy also raises the temperature and subsequently decreases CO₂ density as a result. This complex process requires further examination.

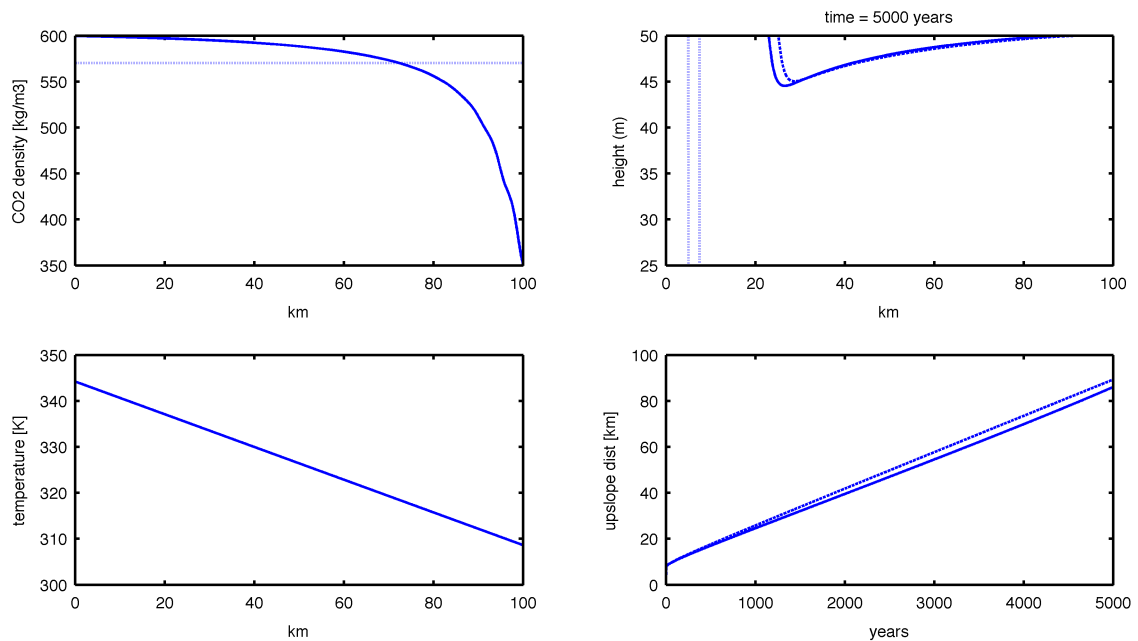


Fig. 2. Sloping aquifer simulation case: (a) left column shows CO₂ density (top) and temperature (bottom); (b) right column shows resulting plume interface with initial condition (top) and upslope extent (bottom); all three cases of density variation are shown: variable density (solid) and constant density (dashed).

5. Summary

In this paper, we present a coupled thermal and VE flow model along with preliminary results for aquifers in which temperature may have a significant impact on CO₂ density. The following observations can be made:

- VE models are well suited for large-scale and long-term storage simulation;
- non-isothermal capability can further extend the applicability of the VE model to more complex systems;
- further investigation is required into the behavior of PVT formulations and extension of cubic equations-of-state to give more reliable CO₂ properties;
- preliminary results show expected CO₂ behavior impacted by temperature, although further work is required to verify the results against fully 3D non-isothermal simulators; and
- the validity of assumptions in the integrated temperature model will be explored in future work.

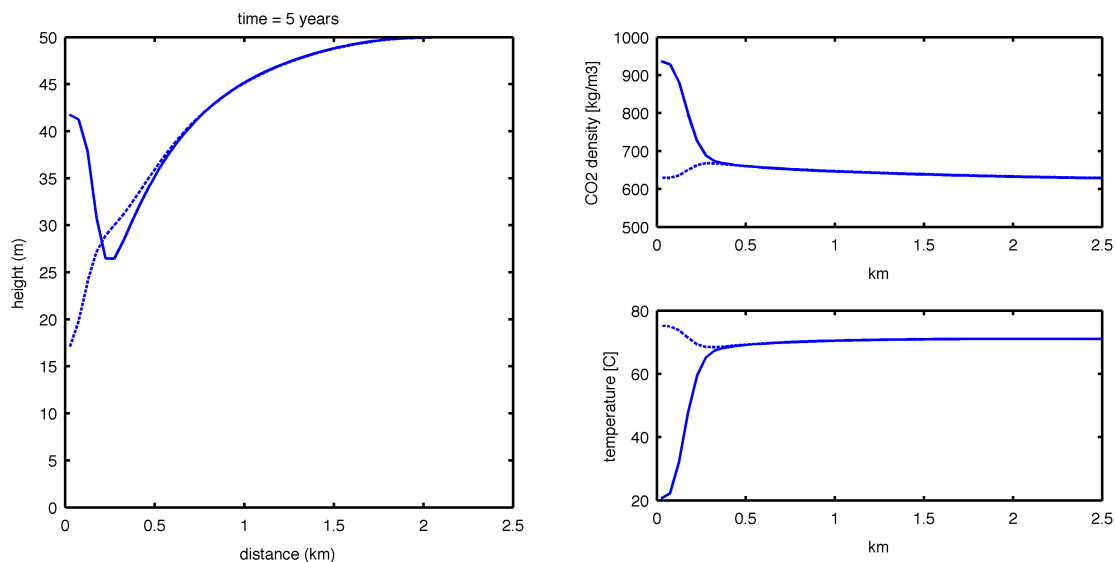


Fig. 3. (a) first column shows resulting plume interface; (b) right column shows CO₂ density (top) and temperature (bottom); two cases injection temperature are shown: 20 C (solid) and 70 C (dashed).

Acknowledgements

This work has been sponsored by the Norwegian Research Council and Statoil ASA through the MatMoRA-II project (project.no. 215641).

References

- [1] Gor, GY, Elliot, TR, Prévost, JH. Effects of thermal stresses on caprock integrity during CO₂ storage. *Int J Greenhouse Gas Contr* 2013;**12**:300–9.
- [2] Nazarian, B, Held, R, Høier, L, Ringrose, P. Reservoir management of CO₂ injection: pressure control and capacity enhancement. in *Proceedings of 11th Int Conf on Greenhouse Gas Technologies, Kyoto, Japan, 2012*;1–11.
- [3] Nordbotten, JM, Celia, MA. *Geological Storage of CO₂: Modeling approaches for large-scale simulation*. New Jersey: Wiley; 2012.
- [4] Nordbotten, JM, Dahle, HK. Impact of the capillary fringe in vertically integrated models for CO₂ storage. *Water Resour Res* 2011;**47**:W02537.
- [5] Gasda, SE, Nilsen, HM, Dahle, HK, Gray, WG. Effective models for CO₂ migration in geological systems with varying topography. *Water Resour Res* 2012;**48**:W10546.
- [6] Gasda, SE, Nordbotten, JM, Celia, MA. Vertically-averaged approaches for CO₂ migration with solubility trapping. *Water Resour Res* 2011;**47**:W05528.
- [7] Aavatsmark, I. *Mathematische Einführung in die Thermodynamik der Gemische*. Berlin: Akademie Verlag; 1995.
- [8] Span, R, Wagner, W. A new equation of state for carbon dioxide covering the fluid region from the triple point temperature to 1100 K at pressures up to 800 MPa. *J Phys Chem RefData*, 1996;**25**:1509–96.